N. Milošević[1], A. Sedmak[2], I. Martić[1], R. Prokić-Cvetković[2]

NOVEL PROCEDURE TO DETERMINE ACTUAL STRESS-STRAIN CURVES
NOVI POSTUPAK ODREĐIVANJA STVARNIH DIJAGRAMA NAPON-DEFORMACIJA

Originalni naučni rad / Original scientific paper
UDK /UDC:

Rad primljen / Paper received: 2.03.2021

Adresa autora / Author's address:
[1)] Innovation Centre of the Faculty of Mechanical Engineering, Serbia, email: nmilosevic@mas.bg.ac.rs
[2)] University of Belgrade, Faculty of Mechanical Engineering, Belgrade, Serbia

Keywords
- stress-strain diagram
- undermatched weld
- digital image correlation (DIC)
- finite element method (FEM)

Abstract

This paper presents a novel procedure for determining the actual stress-strain curves for undermatching rectangular welded joints made of martensitic armoured steel Armox 500T. The method is based on an analytical expression for true stress; digital image correlation (DIC) with two cameras, i.e. recording 3D deformations of samples; and finite element method (FEM) for stress state analysis of samples. Stresses obtained by dividing the force by the current cross-sectional area of the sample do not represent the actual stress occurring in the sample, because they do not take into account the stress concentration. In this paper we have analysed the stress concentration obtained numerically using Abaqus software in which the model's entered strain values are measured by DIC method.

Ključne reči
- dijagram napon-deformacija
- andermečing zavareni spoj
- korelacija digitalne slike (DIC)
- metoda konačnih elemenata (MKE)

Izvod

U ovom radu je prikazana nova metoda za određivanje stvarnih dijagrama napon-deformacija kod andermečing zavarenih spojeva, izvedenih na martenzitnom pancirnom čeliku Armox 500T. Metoda se zasniva na upotrebi analitičke relacije za stvarni napon; korelacije digitalne slike (DIC) sa dve kamere, tj. snimanjem 3D deformacija uzoraka, i metode konačnih elemenata (MKE) za analizu naponskog stanja uzoraka. Naponi dobijeni deljenjem sile sa trenutnom površinom poprečnog preseka uzorka ne predstavljaju stvarni napon, jer se u proračunu ne uzima u obzir koncentracija napona. U ovom radu, koncentracija napona je dobijena numerički upotrebom softvera Abaqus u kojem je analiziran model sa unetim vrednostima deformacija koje su izmerene DIC metodom.

INTRODUCTION

The stress-strain diagram represents a widely used diagram in engineering. Much research tries to determine the true or actual diagram based on analytical expressions, /1-7/, in combination with experiment and numerical simulation. Recent development of optical extensometers and cameras for strain measurement enabled more advanced analysis of strains and stresses, /8-12/. Values for true stress are obtained from the law of mass balance, i.e. from a constant sample volume. This approach gives satisfactory results only for small strain values. At high values of plastic strain, especially after reaching the value of maximum force, this approach does not give precise results because it does not take into account contraction and the creation of a 'neck'. Because of that this stress is named 'true' in this paper. After reaching the maximum force, the neck is formed in the cross-section of a sample, causing significant contraction and triaxial stress state. Many researchers have come to this conclusion and have noticed that a correction of equivalent stress is needed, /2-6/. Stress correction is needed because of stress concentration that occurs at the contracted cross-section of a sample. In this paper values for the stress concentration are introduced analytically and verified numerically, using Abaqus®.

EXPERIMENT

Samples for the experiment are made with V groove weld and cut by waterjet from the plate of the Armox 500T armoured steel. Weld is made with TIG and MMA process. The root and hot pass are made with TIG, and the filling passes with MMA welding process. Chemical composition of the base metal (BM) is given in Table 1.

Table 1. Chemical composition of the BM.

[%]	C	Mn	Si	Ni	Cr	Mo	B	S	P
Armox 500T	0.32	1.2	0.4	1.8	1.0	0.7	0.005	0.003	0.01

Filler materials used for TIG welding are S Ni 6082 (EN ISO 18274), and for the MMA welding: E 19.12.3 Nb R 26 (ISO 3581). Chemical compositions of filler materials are shown in Table 2. Tensile properties for base and filler materials are shown in Table 3. The dimensions of the samples are shown in Fig. 1.

Table 2. Chemical composition of filler materials.

[%]	C	Si	Mn	Cr	Ni	Mo	Nb	Cu	Ti	P	S
S Ni 6082	max 0.01	max 0.1	3.2	20.8	72.9	/	2.5	max 0.1	0.3	0.003	0.001
E 19.12.3 Nb R 26	0.02	0.9	0.7	18.0	12.0	2.7	0.4	max 0.5	/	0.02	0.02

Table 3. Mechanical properties of used materials.

	$R_{p0.2}$ [MPa] min.	R_m [MPa] min.	A_5 [%] min.	KV [J] 20°C
Armox 500T	1250	1450-1750	8	
S Ni 6082	400	min 620	35	min 150
E 19.12.3 Nb R 26	400	min 590	30	min 47

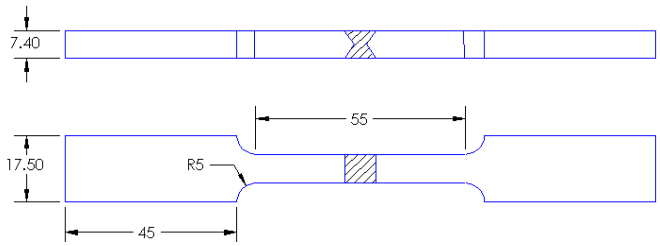

Figure 1. Specimen dimensions.

STRAIN ANALYSIS

Strains are measured by two DIC cameras and extensometer, Fig. 2, to be processed in Aramis software, as shown in Fig. 3, for the stage 125 after 252.12 s.

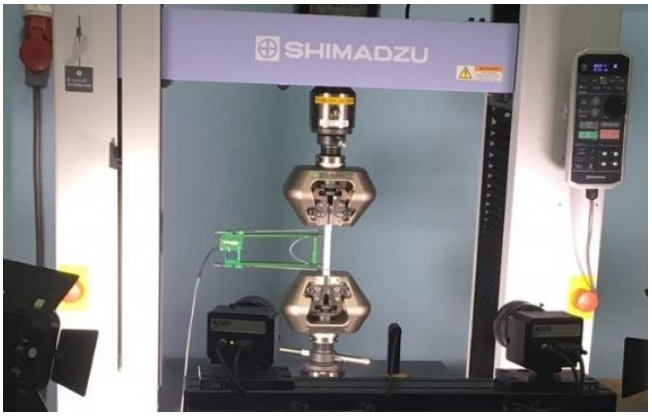

Figure 1. Setup of the cameras and extensometer.

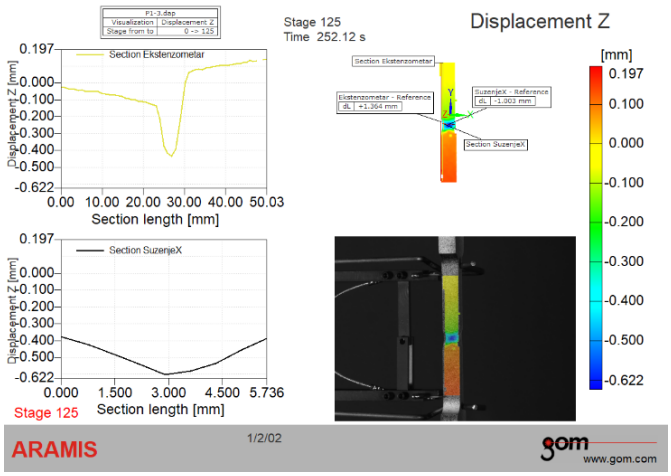

Figure 2. Strain analysis in software Aramis®.

Tables with coordinates of points attached to samples are obtained as a result of analysis in the software. These coordinates are input into SolidWorks as a curve, and assuming that the opposite sides of the specimen deform similarly, the current cross-sectional area of the specimen is obtained. The appearance of the obtained surface is shown in Fig. 3.

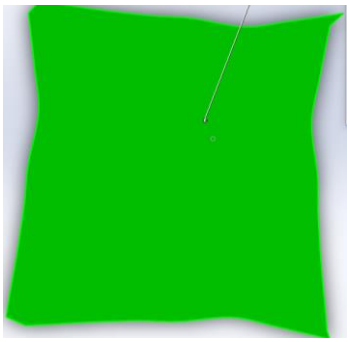

Figure 3. Shape of current cross section of the specimen.

Points of interest are chosen with respect to strain which is measured with extensometer. After 0.2 % of plastic deformation is reached, the area from that point to fracture is divided in sections. The number of sections is conditioned by the size of the obtained area. Minimum of 5 sections are used as a reference. This indicates that for every specimen, a minimum of 5 points are modelled, calculated, and analysed. For all points, the current cross-section is calculated, and maximal coordinate differences are used as vertices of the radius of curvature entered on the model for FEM. In order to obtain actual stress values, regardless of the magnitude of the deformation, the models for FEM analysis already have the deformation measured by DIC. Dimensions are entered along all three axes and deformed models are made.

STRESS ANALYSIS

The analysis of the actual stress the specimen is exposed to are obtained in Abaqus. The deformed models are divided by two symmetry axes and the stress is given by pressure (negative stress). Its value is calculated by force, at that moment, and divided by the maximal cross-section of the specimen. As a finite element, the brick element is used with eight nodes, with the mashing displayed in Fig. 4.

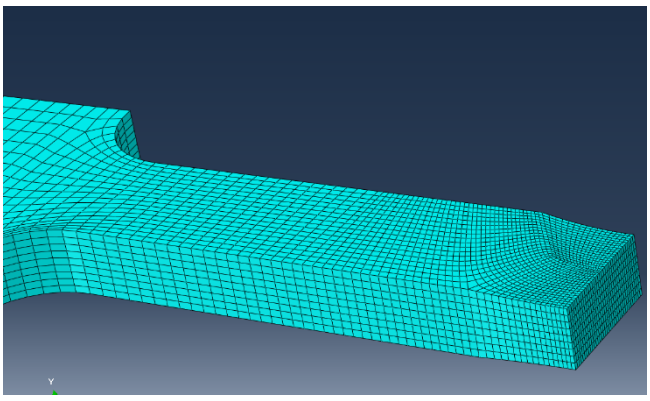

Figure 4. Mash of the modelled P1 specimen.

The stress for comparison is the true stress, calculated by the equation:

$$\sigma_T = \frac{F}{A_{cur}}, \tag{1}$$

where: A_{cur} is current cross-section of the specimen. After a few points of interest being analysed, it is found that the actual stress to which the specimen is exposed to, obtained from Abaqus, is higher than the actual stress calculated by

Eq.(1). This led to the establishing of a new coefficient. The formula for calculating the actual stress is then:

$$\sigma_{\text{actual}} = \sigma_T (C_{ZS} + C_{EP}) , \tag{2}$$

where: C_{ZS} and C_{EP} are coefficients for the weld joint and specimen, in respect. Dimensions that we have taken into account are shown in Fig. 5.

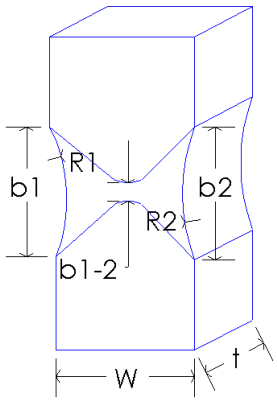

Figure 5. Dimensions for calculating the coefficients.

The actual stress is higher than true stress because of stress concentration occurring at the site of specimen contraction. With this in mind we can determine the coefficient. The stress concentration factor depends exclusively on geometry parameters, as is shown in Fig. 5.

In previous analyses, researchers have always taken into account the radius of curvature R, but also the ligament, which does not affect the stress concentration but only describes the current cross-section area of the specimen. In addition, the ligament is located inside the material, perpendicular to the loading axis, so that it cannot affect the stress concentration on the surface. Therefore, the geometric variables of the welded joint that affect the stress concentration are the dimensions along the load axis, b which is directly proportional to the stress concentration, and is also related to the radius of curvature R which is indirectly proportional to stress concentration (when $R \to 0$, $\sigma \to \infty$). So, the initial form of the C_{ZS} factor is:

$$C_{ZS} = \frac{b}{R} . \tag{3}$$

If we look at this ratio it can be concluded that the ratio will change significantly over time, because with increasing b, the value for R will drop drastically. This phenomenon can be mitigated and at the same time remain in the form of a variable if the value for R in the denominator is added to b which grows over time. So, with this correction, the ratio of these two values does not change so drastically with increasing load. The new form of this part of the coefficient now reads:

$$C_{ZS} = \frac{b}{2(R+b)} . \tag{4}$$

The denominator is multiplied by two due to the narrowing of the specimen along both axes.

Observing the coefficient from Anderson /12/, it can be seen that the stress concentration coefficient has the form:

$$K_A = 1 + \frac{2a}{b} . \tag{5}$$

Therefore, it is necessary to add a constant to the variable coefficients in the form of '1'. The coefficient after this correction takes the form:

$$C_{ZS} = 1 + \frac{b}{2(R+b)} . \tag{6}$$

The part of the coefficient taking account the shape of specimen can now be considered. During the deformation of specimen, the narrowing that occurs across its width is taken into account over the radius of curvature; and the narrowing that occurs across specimen thickness shall not be taken into account. Therefore, in addition to the initial width and thickness of the specimen, a reduction in thickness over time should be included in the coefficient related to specimen shape. Thickness reduction can be considered from the relationship:

$$C_{EP} = \frac{\Delta t}{t_0} . \tag{7}$$

Since it is sometimes necessary to analyse different specimen shapes, we introduce initial dimensions of specimen shape into the coefficient as follows:

$$C_{EP} = \frac{\Delta t / t_0}{2W_0 / t_0} . \tag{8}$$

After arranging the double fraction, we obtain:

$$C_{EP} = \frac{\Delta t}{2W_0} . \tag{9}$$

The full coefficient is then:

$$1 + \frac{b}{2(R+b)} + \frac{\Delta t}{2W_0} . \tag{10}$$

Specimen P1 reaches the value of 0.2 % plastic deformation at stage 60 and the break point occurs at stage 91, given by the DIC. Numerical analysis is done in Abaqus for stages 60 to 90. Values obtained by Abaqus for stage 90 are shown in Fig. 6. Values calculated by Eqs.(1), (2) and (10):

$$\sigma^1_{\text{actual}} = 905.4 \text{ MPa} , \tag{11}$$

$$\sigma^2_{\text{actual}} = 908.6 \text{ MPa} . \tag{12}$$

Differences between stresses calculated analytically and numerically for all points in specimen P1 are given in Table 4.

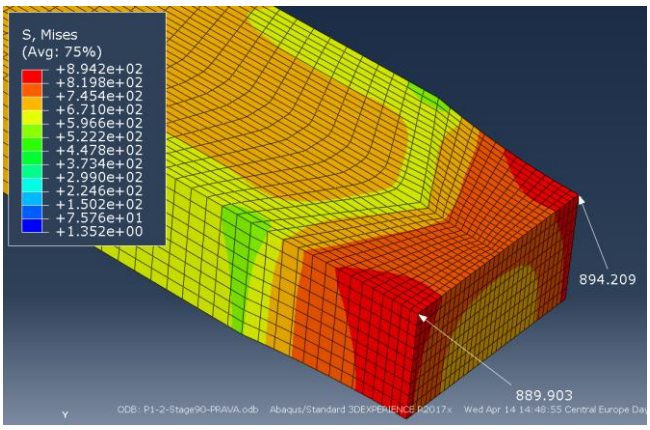

Figure 6. Equivalent stress values for specimen P1, stage 90.

Table 4. Difference in stresses for specimen P1.

Stage	σ^1_{actual} [MPa]	Abaqus 1 [MPa]	Dif. [%]	σ^2_{actual} [MPa]	Abaqus 2 [MPa]	Dif. [%]
60	374.6	373.9	0.19	374.7	373.9	0.20
70	523.8	519.1	0.91	524.3	519.3	0.95
80	690.1	671.7	2.74	691.8	672.7	2.85
90	905.4	889.9	1.74	908.6	894.2	1.61

Maximum difference obtained for specimen P1 is 2.85 % as can be seen in Table 4. The actual diagram for specimen P1 is shown in Fig. 7 along with the engineering- and true stress-strain curves.

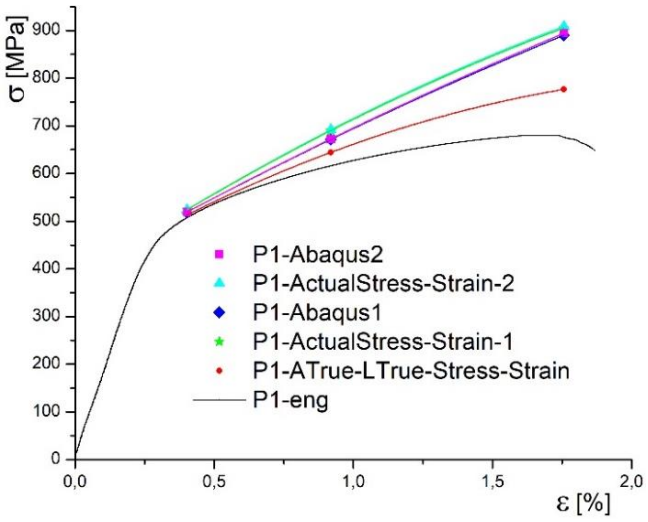

Figure 7. Comparison of the actual, true, and engineering stress-strain curves.

CONCLUSIONS

Actual stresses the specimen is exposed to during the tensile test are much higher than values obtained by standard method. The stresses show that the material has higher strength compared to values marked as ultimate tensile strength.

This procedure shows that actual values of stress in the tensile specimen can be calculated analytically if all the necessary geometric parameters are known.

The difference between Abaqus results and those calculated by analytical formulas are in the range of 3 %.

Further analysis is needed to include different shapes of specimens.

ACKNOWLEDGEMENTS

The results presented are part of a research supported by MESTD RS by contract 451-03-9/2021-14/200105.

REFERENCES

1. Ling, Y. (1996), *Uniaxial true stress-strain after necking*, AMP J Technol. 5: 37-48.
2. Ostsemin, A.A. (1992), *Stress in the least cross section of round and plane specimens in tension*, Strength Mater. 24(4): 298-301. doi: 10.1007/BF00777347
3. Tu, S., Ren, X., He, J., Zhang, Z. , *Experimental measurement of temperature-dependent equivalent stress-strain curves of a 420 MPa structural steel with axisymmetric notched tensile specimens*, Eng. Fail. Anal. 100: 312-321. doi: 10.1016/j.engfailanal.2019.02.043
4. Scheider, I., Brocks, W., Cornec, A. (2004), *Procedure for the determination of true stress-strain curves from tensile tests with rectangular cross-section specimens*, J Eng. Mater. Technol. 126(1): 70-76. doi: 10.1115/1.1633573
5. Yuan, W.J., Zhang, Z.L., Su, Y.J., et al. (2012), *Influence of specimen thickness with rectangular cross-section on the tensile properties of structural steels*, Mater. Sci. Eng. A, 532(15): 601-605. doi: 10.1016/j.msea.2011.11.021
6. Zhang, Z.L., Hauge, M., Thaulow, C., Ødegard, J. (2002), *A notched cross weld tensile testing method for determining true stress-strain curves for weldments*, Eng. Fract. Mech. 69: 353-366. doi: 10.1016/S0013-7944(01)00075-3
7. Cheng, C.H., Jie, M., Chan, L.C., Chow, C.L. (2007), *True stress-strain analysis on weldment of heterogeneous tailor-welded blanks-a novel approach for forming simulation*, Int. J Mech. Sci. 49(2): 217-229. doi: 10.1016/j.ijmecsci.2006.08.012
8. Sedmak, A., Milošević, M., Mitrović, N., Petrović, A., Maneski, T. (2012), *Digital image correlation in experimental mechanical analysis*, Struct. Integ. and Life, 12(1): 39-42.
9. Milošević, M., Mitrović, N., Jovičić, R., et al. (2012), *Measurement of local tensile properties of welded joint using digital image correlation method*, Chemicke listy, 106: s485-s488.
10. Milošević, N., Sedmak, A., Jovičić, R. (2018), *Analysis of strain distribution in overmatching V groove weld using digital image correlation*, Procedia Struct. Integ. 13: 1600-1604. doi: 10.1016/j.prostr.2018.12.337
11. Milošević, M., Milošević, N., Sedmak, S., et al. (2016), *Digital image correlation in analysis of stiffness in local zones of welded joints*, Tehnicki Vjesnik, 23(1): 19-24. doi: 10.17559/TV-20140123151546
12. Anderson, T.L., Fracture Mechanics: Fundamentals and Applications, 4th Ed., CRC Press, 2017.